Acta Crystallographica Section F
Structural Biology and Crystallization Communications
ISSN 1744-3091

Structure of *Escherichia coli* malate dehydrogenase at 1.45 Å resolution

Jelena Zaitseva, Kathleen M. Meneely and Audrey L. Lamb*

Department of Molecular Biosciences, University of Kansas, Lawrence, Kansas 66045, USA

Correspondence e-mail: lamb@ku.edu

Received 22 May 2009
Accepted 13 August 2009

PDB Reference: malate dehydrogenase, 3hhp, r3hhpsf.

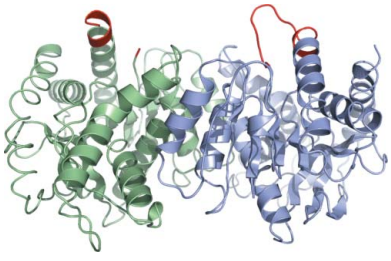

The structure of apo malate dehydrogenase from *Escherichia coli* has been determined to 1.45 Å resolution. The crystals belonged to space group *C*2, with unit-cell parameters $a = 146.0$, $b = 52.0$, $c = 168.9$ Å, $\beta = 102.2^\circ$. The structure was determined with the molecular-replacement pipeline program *BALBES* and was refined to a final *R* factor of 18.6% ($R_{\rm free}$ = 21.4%). The final model has two dimers in the asymmetric unit. In each dimer one monomer contains the active-site loop in the open conformation, whereas in the opposing monomer the active-site loop is disordered.

1. Introduction

Malate dehydrogenase (MDH) is an enzyme of the citric acid cycle that catalyzes the reversible oxidation of malate to oxaloacetate with the concomitant reduction of NADH. In prokaryotes, MDH is a homodimer (McAlister-Henn *et al.*, 1987). Apo and holo structures of *Escherichia coli* malate dehydrogenase have been solved previously (Bell *et al.*, 2001; Hall & Banaszak, 1993; Hall *et al.*, 1992). In the present study, MDH was crystallized unexpectedly as a minor contaminant from a system designed for the overexpression and purification of *Pseudomonas aeruginosa* salicylate adenylase (PchD) in *E. coli*. The crystals believed to be PchD were later identified as MDH using the molecular-replacement pipeline program *BALBES* (Long *et al.*, 2008). The structure determination and refinement were completed because the data were 0.4 Å higher resolution than the highest resolution ligand-bound structure and 0.75 Å higher resolution than the highest resolution apo structure. MDH crystallized with two dimers in the asymmetric unit. Two monomers (one per dimer) are in the open conformation reported by Banaszak and coworkers (Bell *et al.*, 2001), in which the loop comprising residues 79–91 shifts position to expose the substrate-binding pocket. In the other monomer of each dimer this loop was disordered and thus was not apparent in the electron density.

2. Experimental methods

2.1. Protein expression and purification

The plasmid pPchD (Quadri *et al.*, 1999) was a gift from Professor C. T. Walsh (Harvard Medical School). The QuikChange kit (Stratagene) and two primers, 5′-GCG AGC TGG AGG CCC GCG CAT GAC TTG CGG CCG CAC TCG-3′ and 5′-CGA GTG CGG CCG CAA GTC ATG CGC GGG CCT CCA GCT CGC-3′, were used to insert the natural stop codon, thus eliminating the C-terminal histidine tag. *E. coli* BL21 (DE3) (Stratagene) cells were transformed with this variant of the previous plasmid, encoding the wild-type *pchD* gene. A single colony was inoculated into 50 ml Luria–Bertani (LB) medium supplemented with kanamycin (50 µg ml^{-1}) and incubated at 310 K with shaking (250 rev min^{-1}) for 6 h. The culture was harvested by centrifugation (6000*g*, 10 min, 277 K). The pellet was stored at 277 K overnight and resuspended in 2 × 500 ml LB medium supplemented with kanamycin (50 µg ml^{-1}). The cultures were grown at 310 K with shaking (250 rev min^{-1}) until an OD_{600} of 0.8 was reached. The cultures were cooled to 291 K with continued shaking

Table 1
Crystallographic statistics.

Values in parentheses are for the highest resolution shell.

Data collection	
Resolution range (Å)	60.97–1.45 (1.49–1.45)
Space group	*C*2
Unit-cell parameters (Å, °)	a = 146.0, b = 52.0, c = 168.9, β = 102.2
Observations	
Unique	216241
Total	1951316
Mosaicity (°)	0.30
Completeness (%)	98.4 (94.8)
Multiplicity	2.8 (2.2)
$R_{\rm merge}$†	0.056 (0.417)
$\langle I/\sigma(I)\rangle$	11.2 (1.5)
Refinement	
Resolution range (Å)	60.97–1.45
No. of reflections‡	194384
R factor§	0.186
$R_{\rm free}$‡	0.214
No. of atoms	
Protein, non-H	9422
Nonprotein	567
R.m.s. deviations	
Lengths (Å)	0.024
Angles (°)	2.06
Overall B factor (Å^2)	17.6

† $R_{\rm merge} = \sum_{hkl}\sum_i |I_i(hkl) - \langle I(hkl)\rangle|/\sum_{hkl}\sum_i I_i(hkl)$. ‡ 9.9% of the reflections were reserved for calculation of $R_{\rm free}$. § R factor $= \sum_{hkl} ||F_{\rm obs}| - |F_{\rm calc}||/\sum_{hkl}|F_{\rm obs}|$.

and protein expression was induced at an OD_{600} of 0.9 with 0.1 m*M* isopropyl β-D-1-thiogalactopyranoside. The cells were harvested by centrifugation (6000*g*, 10 min, 277 K) after 20 h. The cell pellet was resuspended in 30 ml 20 m*M* Tris–HCl pH 8.5 (lysis buffer).

Cells were disrupted by three passes through a French pressure cell (241 MPa) and the cellular debris was removed by ultracentrifugation (142 000*g*, 2 h, 277 K). The supernatant was dialyzed overnight against lysis buffer and loaded onto a Source 30Q anion-exchange column (GE Healthcare) equilibrated with lysis buffer. PchD and malate dehydrogenase were eluted at approximately 50–75 m*M* NaCl in a linear gradient of 0–125 m*M* NaCl over 20 column volumes. The pooled fractions were loaded onto a Superdex 75 size-exclusion column (GE Healthcare) equilibrated with 100 m*M* *N*-(2-acetamido)-iminodiacetic acid (ADA) pH 7.0. The fractions containing PchD and malate dehydrogenase were pooled, diluted by half with water and concentrated using an Amicon stirred cell with a YM-30 membrane to 26 mg ml^{-1} as determined by the Bradford assay.

2.2. Crystallization, data collection and processing

Malate dehydrogenase was selectively crystallized at 291 K by hanging-drop vapor diffusion. Drops containing 4 µl protein solution pre-incubated with 1 m*M* *p*-chloromercuribenzoate (PCMB) were mixed with 0.5 µl reservoir solution (100 m*M* ADA pH 6.5, 0.2 *M* sodium acetate, 30% PEG MME 5000, 5% glycerol). Rod-shaped single crystals formed in one week and reached full size after two weeks. For data collection, the crystals were washed four times in cryoprotectant containing 100 m*M* ADA pH 7.0, 30% PEG MME 5000, 30% glycerol to remove excess mercury and flash-cooled in liquid nitrogen. Diffraction data were collected on beamline 9-2 at the Stanford Synchrotron Radiation Laboratory (Menlo Park, California, USA) with a wavelength of 1.00 Å at 100 K. The exposure time per frame was 5 s, with a crystal-to-detector distance of 200 mm. A fluorescence scan of the crystal indicated that mercury was not present. The data were processed with *MOSFLM* and *SCALA* (Collaborative Computational Project, Number 4, 1994). The crystals were assigned to space group *C*2, with unit-cell parameters a = 146.0, b = 52.0, c = 168.9 Å, β = 102.2°. Data-collection statistics are given in Table 1.

2.3. Structure determination and refinement

A molecular-replacement search using the program *BALBES* (Long *et al.*, 2008) and the *FASTA* sequence of *E. coli* malate dehydrogenase was completed, yielding a clear solution with one dimer in the asymmetric unit. Inspection of the crystal packing showed gaps in the lattice with electron density corresponding to a second dimer in the asymmetric unit, which was placed with the program *Phaser* (McCoy *et al.*, 2005), fixing the first dimer and searching for the second by molecular replacement. Model building was performed using *Coot* (Emsley & Cowtan, 2004) in iterative cycles with refinement using *REFMAC*5 (Winn *et al.*, 2001). Refinement statistics are given in Table 1. The final model contains two dimers per asymmetric unit. Monomer *A*, composed of residues 1–312, forms a dimer with monomer *B* (residues 1–79 and 87–311). Monomer *C*, composed of residues 1–312, forms a dimer with monomer *D* (residues 1–79 and 85–311). The model includes alternate side-chain conformations for 78 amino acids in the four chains. The model also includes 567 water molecules and no mercury. Waters were added using a $2(F_o - F_c)$ map at 1.5σ. Additional waters could be added to $2(F_o - F_c)$ maps drawn at 1.0σ, thereby lowering the *R*

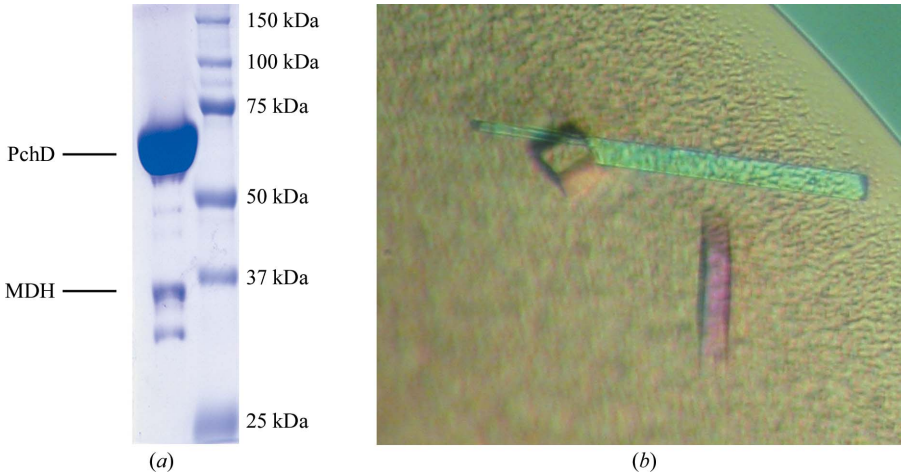

Figure 1
(*a*) SDS–PAGE gel showing protein purity. The protein purified, salicylate adenylase (PchD) from *P. aeruginosa*, also contained the *E. coli* malate dehydrogenase (MDH) contaminant that readily crystallized. (*b*) Crystals of malate dehydrogenase surrounded by protein precipitate, presumably PchD.

and R_{free}; however, further refinement did not support the inclusion of these water molecules since the electron density was poor. A Ramachandran plot generated by *PROCHECK* (Laskowski *et al.*, 1993) showed that the model exhibits excellent geometry, with 94% of the amino-acid residues in the most favorable region and 6% in the additional allowed region.

2.4. Structure analysis

The structural alignments and calculations of the root-mean-square deviations (r.m.s.d.s) were all performed using *LSQMAN* in the *DEJAVU* program package (Kleywegt & Jones, 1997). The atomic coordinates and structure factors have been deposited in the Protein Data Bank, Research Collaboratory for Structural Bioinformatics, Rutgers University, New Brunswick, New Jersey, USA (entry 3hhp).

3. Results and discussion

This project was initiated with the intent of crystallizing and solving the structure of salicylate adenylase (PchD) from *P. aeruginosa* (PAO1), a protein involved in the pyochelin siderophore-production pathway. This protein, which was produced with a C-terminal histidine tag using the pPchD plasmid (Quadri *et al.*, 1999), did not crystallize. Therefore, the tag was removed by the insertion of a stop codon as described in §2 and the protein was again overexpressed and purified from BL21 (DE3) *E. coli*. The PchD protein contained a few minor contaminants that were evident when visualized by Coomassie-stained SDS–PAGE (Fig. 1*a*), but was deemed suitable for crystallization studies.

Protein crystals were produced surrounded by protein precipitate (Fig. 1*b*). Crystals were carefully excised from the precipitate and were of diffraction quality, routinely diffracting to 2.0 Å resolution. Since molecular replacement using *Phaser* (McCoy *et al.*, 2005) with nonribosomal peptide synthetase adenylase homologues [DhbE from *Bacillus subtilis* (May *et al.*, 2002) and PheA from *Brevibacillus brevis* (Conti *et al.*, 1997)] failed and incorporation of selenomethionine was ineffective, heavy-atom techniques were employed. One crystal soaked in *p*-chloromercuribenzoate diffracted to 1.45 Å resolution and a complete data set was collected on Stanford Synchrotron Radiation Lightsource beamline 9-2 (Table 1). A fluorescence scan of the crystal indicated that no mercury was present.

Molecular-replacement calculations were performed using the program *BALBES* (Long *et al.*, 2008) and the *FASTA* sequence for PchD, which yielded no solutions. However, the log file indicated that there was a similar crystal system with the same space group and isomorphous unit-cell parameters in the Protein Data Bank for malate dehydrogenase (PDB code 2pwz). Malate dehydrogenase (MDH) from *E. coli* has a monomer molecular weight of 32.3 kDa (312 amino acids), the approximate molecular weight of the most significant contaminant in the purification (Fig. 1*a*). Since MDH is a housekeeping gene (part of the citric acid cycle), molecular-replacement calculations were repeated using the *FASTA* sequence of MDH. This produced a clear solution, placing one dimer in the asymmetric unit. However, the Matthews coefficient (4.9 Å^3 Da^{-1} for one dimer, 2.45 Å^3 Da^{-1} for two dimers) and the incomplete lattice from this solution indicated that a second dimer should be present.

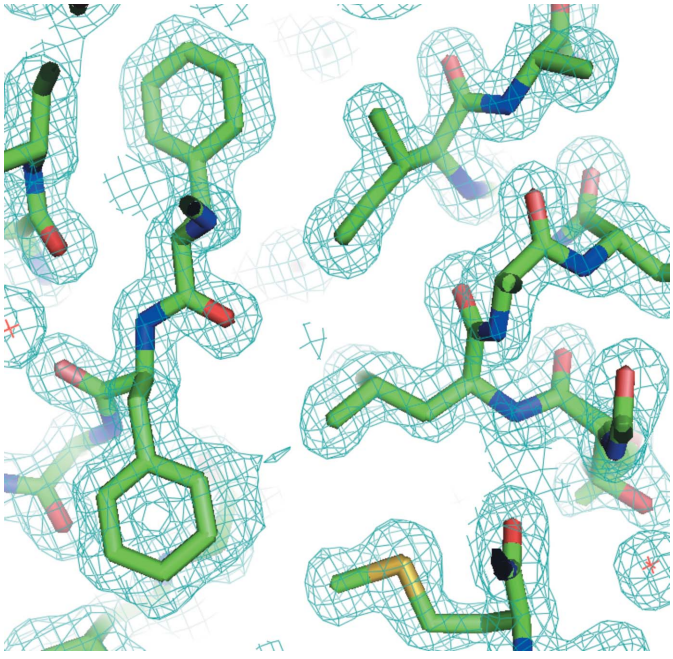

Figure 2
Representative $2F_o - F_c$ electron-density maps contoured at 1σ. The holes in the aromatic amino acids are readily apparent (Phe263 is pointing up and Phe264 is pointing down) and the difference in the size of the S atoms relative to the C, O and N atoms is also evident (Met295).

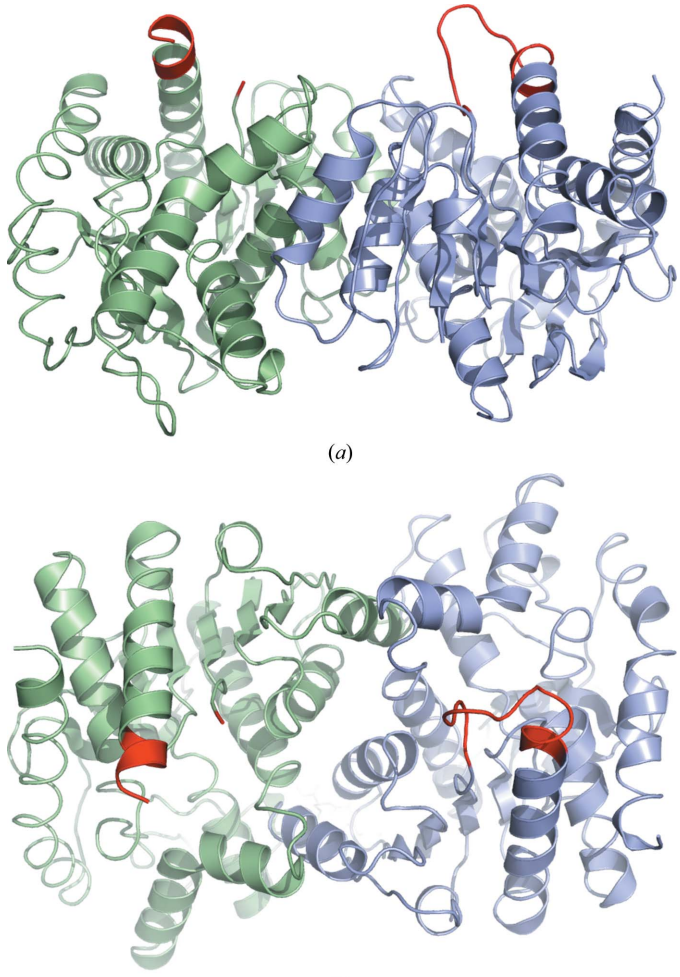

Figure 3
Dimeric structure of *E. coli* malate dehydrogenase. Monomer *A* is shown in blue and monomer *B* is shown in green, with the active site loop in red. The second image is rotated 90° about the *x* axis relative to the first.

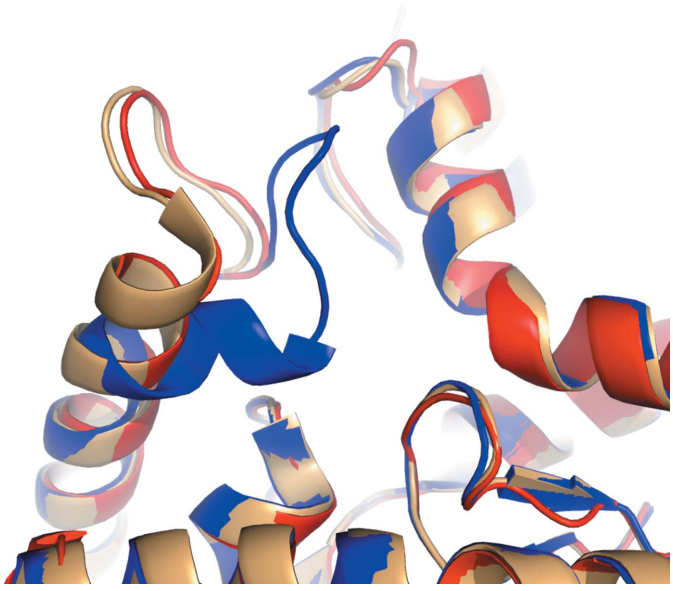

Figure 4
Comparison of the malate dehydrogenase active site (red, monomer *A*) to the previously determined open (tan; PDB entry 1ie3) and closed (blue; PDB entry 1ib6) structures.

This second dimer was easily placed with *Phaser* (McCoy *et al.*, 2005). The refinement of the structure was completed, since this is the highest resolution structure of *E. coli* malate dehydrogenase, and indeed of any malate dehydrogenase, obtained to date. A typical section of electron density can be seen in Fig. 2.

Monomers *A* and *B* form one of the two dimers, whereas as the second dimer comprises monomers *C* and *D*. The dimer composed of monomers *A* and *B* is depicted in two orientations in Fig. 3, with the active-site loops (residues 79–91) shown in red. In each dimer there is one monomer with a well ordered loop, whereas in the second monomer the active-site loop is disordered. None of the monomers contained NAD(H), which is not surprising since this was not a component of the crystallization system, nor is there an ion in the substrate-binding site.

Open and closed active-site *E. coli* MDH structures have been determined previously and closing of the active site is dependent on the inclusion of an ion (citrate, sulfate *etc.*) that can serve as a malate analog: if a malate analog is present, this loop closes over the active site and is held in place by ionic interactions with the ion (Bell *et al.*, 2001; Hall & Banaszak, 1993; Hall *et al.*, 1992). Arg81 has previously been hypothesized to be important for the stability and orientation of the substrate for catalysis and also for substrate specificity (Bell *et al.*, 2001). Superposition of our structure with previously reported structures (PDB entries 1ie3, 1ib6 and 1emd) indicate the expected level of structural similarity. The r.m.s.d. between monomer *A* compared with the previously determined structure with an open active site (PDB code 1ie3) is 0.55 Å for 312 C^{α} atoms (the C^{α} atoms of all amino acids in the protein). A comparison to those with closed active sites (PDB entries 1ib6 and 1emd) shows r.m.s.d. values ranging from 0.62 to 0.65 Å for 304 C^{α} atoms, with those not accounted for being those of residues 80–87, the active-site loop containing the important Arg81 which changes conformation (Fig. 4). In the remaining two monomers (*B* and *D*) of our structure, the active-site loop is disordered and no electron density is visualized for residues 80–86 (*B*) or 80–84 (*D*). The r.m.s.d. for the open structure (1ib6) with monomer *B* gives an r.m.s.d. of 0.51 Å for 304 C^{α} atoms, with the disordered amino acids accounting for the C^{α} atoms not included in the calculation. The structure presented here indicates that there is more mobility in this loop than previously documented.

Diffraction data were collected at the Stanford Synchrotron Radiation Laboratory, a national user facility operated by Stanford University on behalf of the US Department of Energy, Office of Basic Energy Sciences. The SSRL Structural Molecular Biology Program is supported by the Department of Energy, Office of Biological and Environmental Research and by the National Institutes of Health, National Center for Research Resources, Biomedical Technology Program and the National Institute of General Medical Sciences. We would like to thank the staff at the Stanford Synchrotron Radiation Laboratory for their support and assistance. Preliminary X-ray diffraction data were collected at the Protein Structure Lab at the University of Kansas. This study was funded by NIH/NCRR COBRE 5P20-RR17780.

References

Bell, J. K., Yennawar, H. P., Wright, S. K., Thompson, J. R., Viola, R. E. & Banaszak, L. J. (2001). *J. Biol. Chem.* **276**, 31156–31162.
Collaborative Computational Project, Number 4 (1994). *Acta Cryst.* D**50**, 760–763.
Conti, E., Stachelhaus, T., Marahiel, M. A. & Brick, P. (1997). *EMBO J.* **16**, 4174–4183.
Emsley, P. & Cowtan, K. (2004). *Acta Cryst.* D**60**, 2126–2132.
Hall, M. D. & Banaszak, L. J. (1993). *J. Mol. Biol.* **232**, 213–222.
Hall, M. D., Levitt, D. G. & Banaszak, L. J. (1992). *J. Mol. Biol.* **226**, 867–882.
Kleywegt, G. J. & Jones, T. A. (1997). *Methods Enzymol.* **277**, 525–545.
Laskowski, R. A., MacArthur, M. W., Moss, D. S. & Thornton, J. M. (1993). *J. Appl. Cryst.* **26**, 283–291.
Long, F., Vagin, A. A., Young, P. & Murshudov, G. N. (2008). *Acta Cryst.* D**64**, 125–132.
May, J. J., Kessler, N., Marahiel, M. A. & Stubbs, M. T. (2002). *Proc. Natl Acad. Sci. USA*, **99**, 12120–12125.
McAlister-Henn, L., Blaber, M., Bradshaw, R. A. & Nisco, S. J. (1987). *Nucleic Acids Res.* **15**, 4993.
McCoy, A. J., Grosse-Kunstleve, R. W., Storoni, L. C. & Read, R. J. (2005). *Acta Cryst.* D**61**, 458–464.
Quadri, L. E., Keating, T. A., Patel, H. M. & Walsh, C. T. (1999). *Biochemistry*, **38**, 14941–14954.
Winn, M. D., Isupov, M. N. & Murshudov, G. N. (2001). *Acta Cryst.* D**57**, 122–133.